J. Chem. Sci. Vol. 128, No. 7, July 2016, pp. 1057–1066.
DOI 10.1007/s12039-016-1116-y

Copper(II) Schiff base complexes and their mixed thin layers with ZnO nanoparticles

MAGDALENA BARWIOLEK*, ROBERT SZCZĘSNY and EDWARD SZŁYK
Faculty of Chemistry, Nicolaus Copernicus University in Torun, 87-100 Torun, Poland
e-mail: mbarwiolek@umk.pl

MS received 3 March 2016; revised 4 May 2016; accepted 24 May 2016

Abstract. Cu(II) complexes with Schiff bases derived from ethylenediamine (en) and 2-pyridinecarboxaldehyde (pyca), 2,5-dimethoxybenzaldehyde (dmbaH) or 4-imidazolecarboxaldehyde (4Him) were obtained and studied by elemental analysis, UV-VIS and IR spectra. Zinc oxide was synthesized using a simple homogeneous precipitation method with zinc acetate as a starting material. Thin layers of the studied Cu(II) complexes were deposited on Si(111) or ZnO/Si(111) substrates by a spin coating method and characterized with a scanning electron microscopy (SEM/EDS), atomic force microscopy (AFM) and fluorescence spectroscopy. For Cu(II) layers the most intensive fluorescence bands due to intra-ligand transitions were observed between 462 and 503 nm. The fluorescence intensity of thin layers was corelated to the rotation speed. In the case of the $[Cu(II)(en(4Him)_2)Cl_2]$(**2a**)/ZnO/Si and $[Cu(en(dmbaH)_2)Cl_2]$(**3a**)/ZnO/Si layers the quenching of the emission band from ZnO at 440 nm (λ_{ex} = 330 nm) associated with various intrinsic or extrinsic lattice defects was noted.

Keywords. Thin layer; ZnO nanoparticles; copper complexes; AFM; SEM; fluorescence.

1. Introduction

Study of copper(II) complexes of Schiff bases and nitrogen donor ligands has become a focal point of interest for researchers in recent times, not only for their varied structural features, but also for their potential application in various fields.[1–5] These compounds are also known for their biological role and fluorescence properties. For instance, the copper(II) complexes with Schiff bases derived from *trans* (±)cyclohexanediamine and 2-pyridinecarboxaldehyde exhibited luminescence properties in the solution and in the solid state.[6] The Cu(II) complexes $[Cu(II)(L)](CF_3SO_3)_2$, where L is a ligand obtained from cyclohexanediamine or ethylenediamine and aldehydes e.g., 2-quinolinecarboxaldehyde, 6-methyl-2-pyridinecarboxaldehyde or 2-thiazolecarboxaldehyde can be used as molecular memories for the wet chemical computers.[7] Furthermore, Schiff base derivatives incorporating a fluorescent moiety are a useful tool for optical sensing of metal ions. Thin organic and organometallic films have attracted research interest due to their technologically important optical and electronic properties.[8] These materials exhibit luminescence; they are used as conductors, semi-conductors and organic light emitting diodes (OLED).[9–11] Many thin films of metal complexes, such as Zn(II), Pt(II), Cu(II) or Ag(I) with Schiff bases (e.g., N,N′-bis(salicyli dene)-1,2-ethylenediamine, bis(2-(2-hydroxyphenyl) benzothiazole) were synthetised and their luminescence properties have been employed in organic optoelectronics.[12–15]

The thin organic-inorganic layers of different metal compounds were obtained by many different methods e.g., laser ablation, cathodoluminescence or spin coating.[16–19] However, there are only a few reports on copper(II) complexes in materials obtained by spin coating method. For example, $[Cu_3(opba)(pmdta)_2](NO_3)_2$ (pmdta = 1,1,4,7,7-pentamethyl-diethylenetriamine, opba = orthophenylenebis(oxamato)) complex was used to get thin layer of Cu(II) complex on SiO_2/Si.[10] This technique was also used for deposition of $[(n\mathrm{Bu_3P})_3\mathrm{Cu\text{-}O_2CCH_2CO_2\text{-}Cu}(\mathrm{P}n\mathrm{Bu_3})_3]$ and $[(n\mathrm{Bu_3P})_3\mathrm{Cu\text{-}O_2C(CH_2)_2CO_2\text{-}Cu}(\mathrm{P}n\mathrm{Bu_3})_3]$ on SiO_2/TiN/Cu substrate. The layers were then heated up to 450°C, and the result of this process was the conversion of complexes to CuO by decomposition.[20] In this case, SEM results showed incomplete homogeneous layers and defects in the surface structure. This was explained by the different film thicknesses obtained during the spin coating process, which upon heating produced defects due to unequal evaporation leading to partially cracked copper oxide films. These

*For correspondence

results showed the spin coating as a promising method for deposition of thin and homogeneous layers of transition metal complexes. Previously, copper(II) and nickel(II) complexes with optically active Schiff bases derived from (1*R*, 2*R*)(-)cyclohexanediamine or 2-(2-aminoethyl)pyridine were deposited by us on silicon or glass using the spin coating method.[21–23] The obtained thin materials exhibited fluorescence, which depends on the spin coating parameters and the molecular structure of the complexes.

It is also known, that the ZnO layers can be obtained by sputtering processes, pulsed laser deposition technique or by chemical methods such as, microemulsion, hydrothermal, sol-gel and precipitation followed by the deposition of nanoparticle suspensions using wet coating methods.[24–28] Those materials were also used in optical technology. Moreover, the deposited ZnO nanopowders[29,30] and ZnO nanoparticles doped by different metal ions such as, manganese[31] or copper exhibited photoluminescence bands, and the emission intensity increased with increase in doping up to a certain percentage of Cu^{2+} (5%).[32,33]

The advantages of using wet coating method are two-fold: First, the layers can be formed by subsequent or simultaneous deposition of different materials. Second, use of spin coating offers the opportunity for facile fabrication of a uniformly dispersed nanoparticles or/and solutions onto the substrates even for large areas, and well-defined thickness of films in mild conditions. Therefore, this type of deposition method allows to fabricate a wide variety of composite materials. The facts mentioned above: the fluorescence properties of the Schiff bases and their complexes, the possibility of using the spin coating technique for deposition of the copper(II) complexes and ZnO nanoparticles on different substrates and the likely fluorescence behavior of the obtained layers, prompted us to synthesize a series of new copper(II) complexes with Schiff bases derived from ethylenediamine and several aldehydes. These complexes were characterized spectroscopically and their fluorescence properties were also studied.

In this article, we would like to report how a simple and efficient method as spin coating can be utilized to produce composite films using both nanoparticle dispersions and solutions of complexes. Moreover, the aim of the study was to investigate the microstructural and spectroscopic properties of obtained layers. Therefore, the new copper(II) complexes were used as precursors of thin layers in the spin coating technique. In addition, the zinc oxide and the Cu(II) complexes layers doped with ZnO nanopowder were obtained. The morphology and homogeneity of the layers were analyzed by AFM and SEM microscopy, and the fluorescence properties of the layers were studied. The mechanical properties of some layers induced by microindentation were investigated as well.

2. Experimental

2.1 *Materials and methods*

The ethylenediamine (en) (99%), 2-pyridinecarboxaldehyde (99%) (pyca), 2,5-dimethoxybenzaldehyde (dmbaH) (99%), 4-imidazolecarboxaldehyde (4Him) (98%) and ethylene glycol (EG) (99%) were purchased from Aldrich. $CuCl_2{\cdot}2H_2O$, $Cu(OOCCH_3)_2{\cdot}H_2O$ and $Zn(OOCCH_3)_2{\cdot}2H_2O$ were purchased from POCh Gliwice. All reagents were used without further purification.

Infrared spectra were recorded on a Perkin Elmer SPECTRUM 2000 spectrophotometer. UV-Vis absorption spectra were recorded on a Milton Roy Spectronic 1201 spectrophotometer in CH_3CN (1×10^{-5} M) solution. IR spectra were performed on a Spectrum 2000 Perkin/Elmer FT IR using KBr discs in the range 400–4000 cm^{-1} and polyethylene IR sample cards in the range 400-20 cm^{-1}. 13C CPMAS NMR and ^{1}H, ^{13}C, ^{15}N NMR spectra were collected with Bruker AMX - 300 spectrometer (300 MHz) in $CDCl_3$ against TMS. The fluorescence spectra were recorded on a spectrofluorometer F-7000 HITACHI in the range 900–200 nm (5×10^{-4} mol dm^{-3} MeCN solution or silicon slides) Elemental analyses were carried out using a Elementar Gmbh Vario Macro CHN analyzer. The films were deposited on Si(111) wafers (10\10 mm) ~500 um thick using spin coating technique. Precursors were dissolved in tetrahydrofuran and deposited on Si(111) (900–2000 rpm/30 s–600 s; drying 5000 rpm/200 s, 1×10^{-3} M in THF) using a Laurell 650SZ spin coater. Zinc oxide layers were obtained from ethanol suspension (1.2 mg/cm^3) by the same method. A suspension of ZnO was spun onto the substrate at 1000–5000 rpm for 20–360 s and each plate was subsequently dried at a rotation speed of 5000 rpm for 20 s.

The morphology and composition of the obtained materials were analyzed with a scanning electron microscopy (SEM) LEO Electron Microscopy Ltd, England, model 1430 VP equipped with detectors of secondary electrons (SE) and energy dispersive X-ray spectrometer (EDS) Quantax with detector XFlash 4010 (Bruker AXS microanalysis GmbH). The atomic force microscopy AFM studies in the tapping mode were performed on Veeco (Digital Instrument) microscope Type: MultiMode NanoScope IIIa. Powder X-ray diffraction (PXD) analysis was performed using a

Philips (Almelo, The Netherlands) XPERT θ–2θ diffractometer with CuKα radiation. The indentation properties of the layers were made on NHT2 microindentation tester (TTX-NHT) from Anton Paar TriTec SA with a Berkovich indenter using loads 20 and 100 mN and holding time of 5 s. The system hardness and elastic modulus were determined from the indentation curves by the standard Oliver and Pharr method.[34]

2.2 *Synthesis*

2.2a *Synthesis of en(pyca)$_2$* (**1**): Ethylenediamine (en) (60 μL, 1 mmol) in EtOH was added to pyridine-2-carboxaldehyde (pyca) (190 μL, 2 mmol). The mixture was stirred under reflux for 2 h. The orange precipitate formed was recrystallized from ethanol. (82.7% yield). ^{1}H NMR [ppm]: δ 8.62 (d, 2H, arom.), 8.42 (s, 2H, CH=N), 7.98 (d, 2H, arom.), 7.73 (2H, arom.), 7.30 (ddd, 2H, arom.), 4.07 (s, 4H, -CH_2-). ^{13}C NMR [ppm]: δ 163.4 C2, 154.4 C3, 149.4 C7, 136.5 C5, 124.7 C6, 121.3 C4, 61.3 C1(CH_2). ^{15}N NMR [ppm]: -42.5 N(1), -67.3 CH=N. IR (KBr, cm^{-1}): 3010-3070s ν(C-HAr), 2922, 2853s ν(CH), 1645m ν(C=N), 1584s ν(C-N), 1434m ν(C=C).[6,35–40] (vs, very strong; s, strong; m, medium; w, weak, vw ver weak) (figure 1).

UV-visible in MeCN [λ_{max}/nm(ε/[dm^3·mol^{-1}· cm^{-1}])] 235(37520), 267(38120), 319(25326).

2.2b *Synthesis of en(4Him)$_2$* (**2**): (92.1% yield, (60 μL, 1 mmol en, 0.1922 g, 2 mmol 4Him). ^{13}C CP MAS NMR [ppm]: δ 156.1 C2, 139.4 C5, 128.6 C3, 123.6 C4, 62.2 C1(CH_2). IR (KBr, cm^{-1}): 3436w ν(N-H), 2913–3032w ν(-CH), 1648vs ν(C=N), 1512s ν(C-N), 1450vs, 1472m ν(C=C).[6,35–37,41] UV-visible in MeCN [λ_{max}/nm (ε/[dm^3· mol^{-1}· cm^{-1}])] 273(31520), 318(16437) (figure 1).

2.2c *Synthesis of en(dmbaH)$_2$* (**3**): yield (92.2%, 60 μL, 1 mmol en, 0.3323 g, 2 mmol 4Him. ^{1}H NMR [ppm]: δ 8.71 (s, 2H, CH=N), 7.51 (d, 2H), 6.95 (dd, 2H), 6.85 (d, 2H), 3.99 (s, 4H, -CH_2-), 3.82 (s, 6H) 3.79 (s, 6H) ^{13}C NMR [ppm]: δ 158.6 C2, 153.8 C5, 153.4 (C8), 125.3 C3, 118.6 C6, 112.7 C7, 110.6 C4, 61.9 C1(CH_2), 56.3 C10(OCH_3), 55.8 C9(OCH_3). ^{15}N NMR [ppm]: -69.6 -CH=N. IR (KBr, cm^{-1}): 3309 vs ν(N-H), 3009–3064m ν(C-HAr), 2906, 2831s ν(CH), 1637vs ν(C=N), 1582s ν(C-N), 1427s, 1496s ν(C=C), 1303s ν(Ph-O).[36,37,42,43] UV-visible in MeCN [λ_{max}/nm (ε/[dm^3·mol^{-1}·cm^{-1}])] 222(49732), 251(29946), 332(15508) (figure 1).

2.3 *Synthesis of the Cu(II) complexes*

2.3a *[Cu(en(pyca)$_2$)Cl$_2$]* (**1a**): Ethanolic solution of $CuCl_2$ x $2H_2O$ (0.0287 g, 0.16 mmol in 40 mL ethanol) was added to en(pyca)$_2$ (**1**) (0.0396 g (0.16 mmol) in EtOH. The reaction mixture was stirred at 25°C for 4 h, then, the solvent was removed under reduced pressure and a dark green solid was isolated. [Cu(en(pyca)$_2$)Cl$_2$] (**1a**) (Yield 72.8%) Analysis: Calculated for $C_{14}H_{14}N_4Cl_2Cu$: Cu 17.04, C 45.11, H 3.78, N 15.03. Found: Cu 16.61, C 45.48, H 4.11, N 15.34 [%]. IR (KBr, cm^{-1}): 3386 m ν(N-H), 3068 m ν(C=CH), 2922m ν(C-H), 1604vs ν(C=N), 1569m ν(C-N), 1447s ν(C=C), 303s ν(Cu-Cl), 422s ν(Cu-N).[37] UV-visible in MeCN [λ_{max}/nm (ε/[dm^3· mol^{-1}· cm^{-1}])] 255(8461), 320(2307).

In the same way [Cu(en(pyca)$_2$)(OOCCH$_3$)$_2$] (**1b**), [Cu(en(4Him)$_2$)Cl$_2$] (**2a**) and [Cu(en(dmbaH)$_2$)Cl$_2$] (**3a**) were synthesized (figure 1).

2.3b *[Cu(en(pyca)$_2$)(OOCCH$_3$)$_2$]* (**1b**): (79.2% yield, 0.03194 g 0.16 mmol Cu(OOCCH$_3$)$_2$ x H_2O, 0.0396 g 0.16 mmol en(pyca)$_2$). Analysis: Calculated for $C_{18}H_{20}N_4O_4Cu$: Cu 15.13, C 51.48, H 4.80, N 13.34; Found: Cu 15.19, C 51.68, H 4.29, N 13.04 [%]. IR (KBr, cm^{-1}): 3422m ν(OH), 3074w ν(C=CH), 1598vs ν(C=N), 1547vw ν(C-N), 1444m ν(C=C), 1710s ν_{asCOO^-}, 1476m ν_{sCOO^-}, 1292m ν(C-O), 92w4 δ(O-H), 550m ν(Cu-O), 454m ν(Cu-N).[6,7,36,37,44] UV-visible in MeCN [λ_{max}/nm (ε/[dm^3·mol^{-1}·cm^{-1}])] 210(37795), 252(6299), 326(1574).

2.3c *[Cu(en(4Him)$_2$)Cl$_2$]* (**2a**): (84.50% yield, $CuCl_2$ x $2H_2O$ 0.0287 g, 0.16 mmol, 0.03459 g, 0.16 mmol en(4Him)$_2$). Analysis: Calculated for $C_{10}H_{12}N_6Cl_2Cu$: Cu 18.12, C 34.24, H 3.44, N 23.96; Found: Cu 18.13, C 34.48, H 3.12, N 23.71 [%]. IR (KBr, cm^{-1}): 3422m ν(N-H), 2931w, 2853m ν(CH), 1635vs ν(C=N), 1508w ν(C-N), 1438s ν(C=C), 313m ν(Cu-Cl), 458 w ν(Cu-N).[42,45] UV-visible in MeCN [λ_{max}/nm (ε/[dm^3· mol^{-1}· cm^{-1}])] 264(9122), 322(1403).

2.3d *[Cu(en(dmbaH)$_2$)Cl$_2$]* (**3a**): (76.4% yield, $CuCl_2$ x $2H_2O$ 0.0287 g, 0.16 mmol, 0.05702 g, 0.16 mmol en(dmbaH)$_2$). Analysis: Calculated for $C_{20}H_{24}N_2O_4Cl_2Cu$: Cu 12.94, C 48.93, H 3.92, N 5.70; Found: Cu 13.36, C 48.64, H 4.02, N 5.39 [%]. IR (KBr, cm^{-1}): 3307vs ν(N-H), 3009-3064vs ν(C-HAr), 2953, 2967vs ν(CH), 1654vs ν(C=N), 1587vs ν(C-N), 1453s, 1496s ν(C=C), 477w ν(Cu-N), 373s ν(Cu-Cl).[6,34]

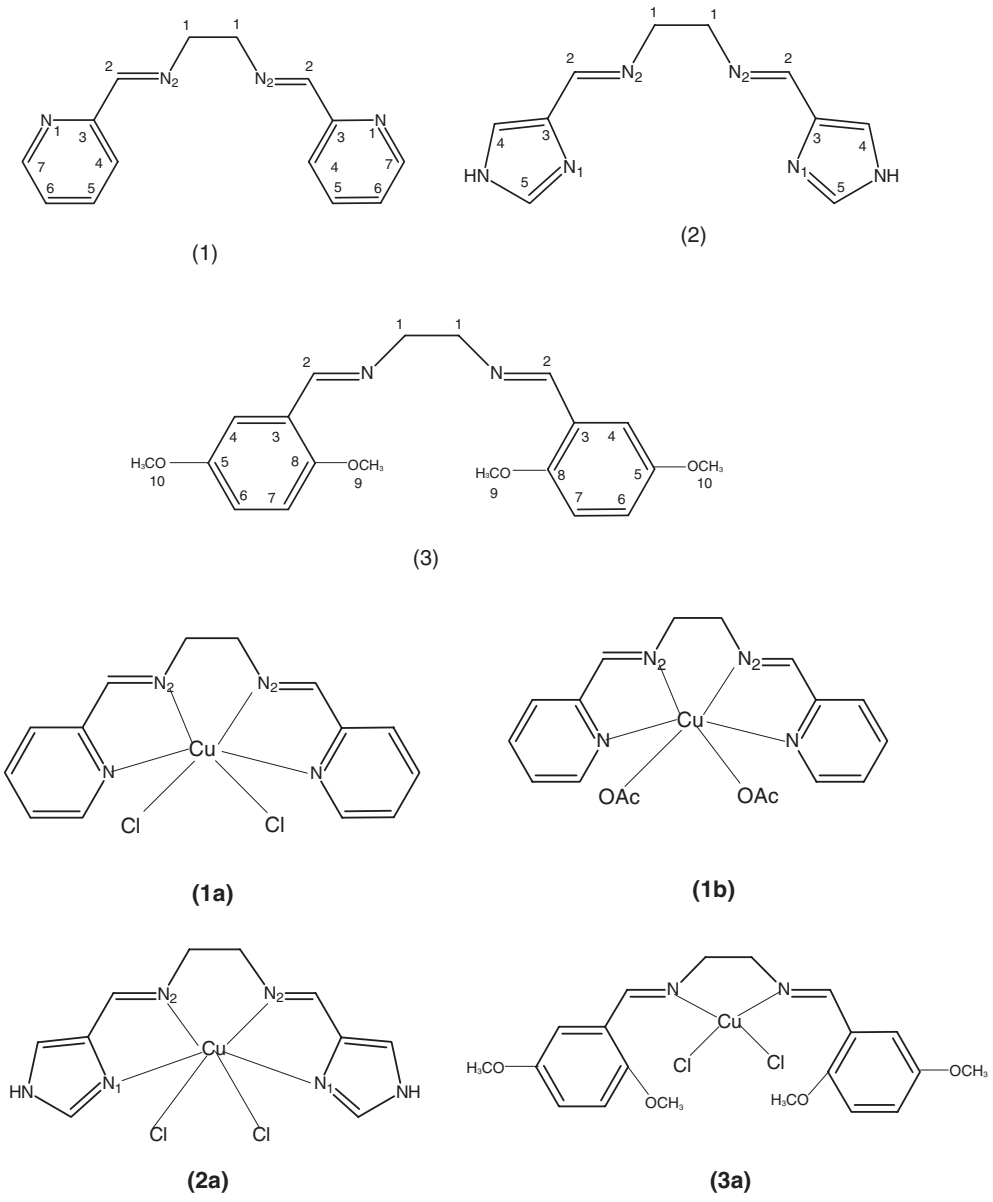

Figure 1. Structures of en(pyca)$_2$ (**1**), en(4Him)$_2$ (**2**) and en(dmbaH)$_2$ (**3**) ligands and copper(II) complexes: [Cu(en(pyca)$_2$)Cl$_2$] (**1a**), [Cu(en(pyca)$_2$)(OOCCH$_3$)$_2$] (**1b**), [Cu(en(4Him)$_2$)Cl$_2$] (**2a**) and [Cu(en(dmbaH)$_2$)Cl$_2$] (**3a**).

UV-visible in MeCN [λ_{max}/nm (ε/[dm^3·mol^{-1}·cm^{-1}])] 211(45098), 251(18627), 350(3921).

2.4 *Synthesis of ZnO nanoparticles*

In a typical synthesis procedure, Zn(OOCCH$_3$)$_2$·2H$_2$O (0.649 g, 3 mmol) and urea (0.995 g, 9 mmol) were added to water/EG solution (1:8 v/v, 75 mL) and kept under stirring solutions at 25°C until a homogeneous solution was obtained. The resultant solution was heated to 90°C. The conditions were kept for 1.5 h and then the mixture was cooled to room temperature. The resulting white precipitate was washed and centrifuged at 9000 rpm with water, acetone and ethanol. Table 1 shows the different experimental condition applied for ZnO preparation.

Table 1. Experimental conditions for ZnO synthesis.

Sample	R	T (°C)	Time (h)
A1	6:1	90	1.5
A2	3:1	70	1.5
A3	3:1	70	3
A4	3:1	90	1.5
A5	1:1	90	1.5
A6	4:1	90	1.5

R = urea/Zn $^{2+}$ molar ratio.

3. Results and Discussion

3.1 *Infrared spectroscopy*

The band from stretching vibrations of the -C=N- group, characteristic of the Schiff base, appeared in the region between 1637 and 1648 cm^{-1}. The band of ν(C=N) vibrations are shifted by 13–41 cm^{-1} in the spectra of copper(II) complexes towards lower frequencies, as a result of Cu(II) coordination with the ligand *via* the azomethine group.[6,45] In the IR spectrum of [Cu(en(pyca)$_2$)(OOCCH$_3$)$_2$] (**1b**) bands at 1475 and 1711 cm^{-1} due to symmetrical and asymmetrical stretching vibrations of acetate ion were observed.[44–48] In (**1b**) the monodentate coordination of CH_3COO^- anion was noted. The similar type of coordination was observed for the copper(II) complex with en(pyca) and CF_3SO_3 ions[7] or Cu(II) and *trans* (±)chxn(pyca).[6] Furthermore, in the spectra of (**1a**), (**2a**) and (**3a**), the band between 303 and 373 cm^{-1} are present due to the stretching vibration of the Cu-Cl in these complexes.[48] Additionally, in the IR spectrum of [Cu(en(pyca)$_2$)(OOCCH$_3$)$_2$] (**1b**), the band from Cu-O vibration at 550 cm^{-1} was observed. Moreover, because of the coordination *via* nitrogen, bands from Cu-N vibrations appeared in the 422–477 cm^{-1} regions in the spectra of all complexes.[6,48] Similar way of coordination was already observed by us in the copper(II) complexes with Schiff bases derived from 2-(2-pyridyl)ethylamine.[23]

The shift of the bands from stretching vibrations of the azomethine group in all the compounds and the presence of specific bands of the Cu-Cl or $COO^-_{asym}/_{sym}$ vibrations in the spectra of particular complexes indicated the correctness of the proposed coordination sphere.

3.2 *Electronic absorption spectra*

All ligands exhibit intense absorption bands between 222 and 273 nm assigned to intraligand $\pi \rightarrow \pi^*$ transition in imidazole or phenolate moieties.[38,49] Moreover, the most characteristic band derived from $\pi \rightarrow \pi^*$ transition in the azomethine group appeared at 319 nm for (**1**), 318 nm for (**2**) and 332 nm for (**3**). The UV-Vis spectra of the complexes showed absorption between 320–350 nm, which can be attributed to a LMCT transitions. Additionally, in the spectra of the complexes, the band from intraligand $\pi \rightarrow \pi^*$ transition in imidazole and phenolate shifted and appeared between 210 nm and 264 nm.

3.3 *ZnO nanoparticles characterization*

The results (figure 2) demonstrated the presence of particles with different particle sizes and shapes, depending on the precipitation conditions. The most homogeneous material with the smallest particle size (sample **A4**) was stick-like in shape with widths of 40 nm and lengths of 100 nm (figure 2a). The other crystallites reach the size of few hundred nanometers (figure 2a, c). The XRD patterns of powders show a full set of diffraction peaks of hexagonal wurtzite structure (JCPDS 36-1451; figure 3a). These data were also confirmed by IR spectra of the prepared samples. A strong band at 422 cm^{-1} with a visible shoulder at 554 cm^{-1} corresponding with Zn-O vibrational mode was observed (figure 3b).[50] Moreover, infrared spectroscopy confirms the presence of functional groups at the surface of ZnO particles. The broad absorption peaks at 3384 cm^{-1} and 2957/2925/2853 cm^{-1} are attributed to stretching vibrations of -OH or -NH groups and the CH stretching, respectively.[51] The bands at 1585 and 885 cm^{-1} are ascribed to in and out of plane of O-H and C=O stretching vibration.[52,53] The absorbance peaks at 1420, 1064 and 1037 cm^{-1} in ZnO can be ascribed to C-O vibration and C-H bending modes. The small bands at 2371 and 2341 cm^{-1} may arise from the absorption of carbon dioxide.

3.4 *Thin films of Cu complexes*

The SEM images of the Cu(II) complex layers showed a uniform distribution of the compounds on the silicon

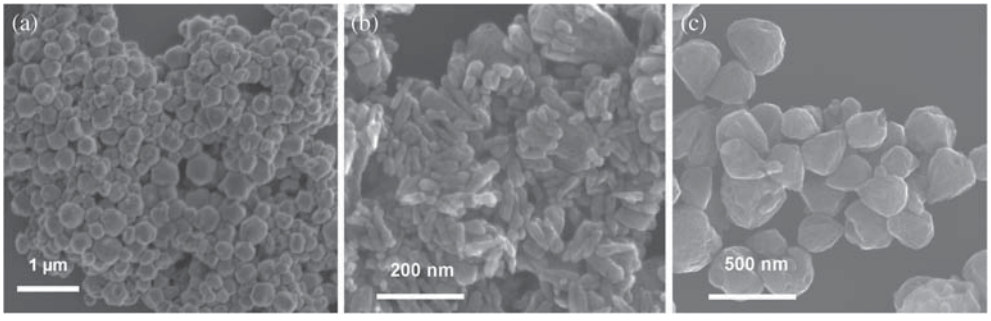

Figure 2. SEM micrographs of ZnO powders: a) sample **A1**, b) sample **A4**, c) sample **A5**.

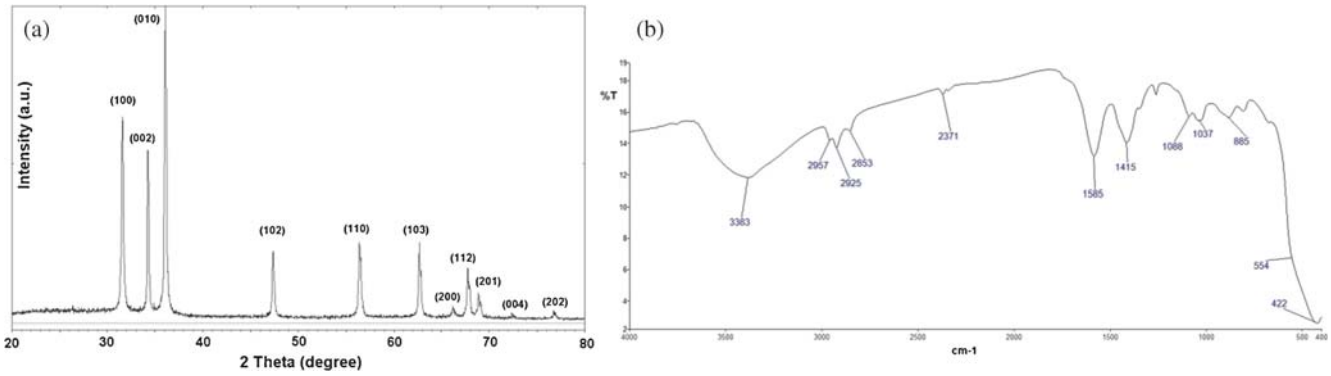

Figure 3. (a) XRD pattern of sample **A4** and (b) IR spectra of sample **A6**.

surface. The layers were amorphous, but small crystallites appeared in some places due to incomplete solidification of the complex solution during the spin coating process, as previously reported.[20,54]

In the case of $Cu(en(pyca)_2)Cl_2]$ (**1a**)/Si and $[Cu(en(dmbaH)_2)Cl_2]$ (**3a**)/Si materials, the whole silicon surface was covered regularly with copper complexes (900, 1100 and 2000 rpm/min (**1a**)/Si and 1000, 1100 and 2000 rpm/min (**3a**)/Si). The EDS results confirmed the presence of copper (0.45% - 900 rpm, 0.71% - 1000 rpm and 0.47% - 1100 rpm) in all (**1a**)/Si layers. Whereas, the $[Cu(en(4Him)_2)Cl_2]$ (**2a**)/Si material exhibited the highest copper content (3.11%) when spin rate 2000 rpm was set.

The SEM/EDS analysis of $[Cu(en(pyca)_2)(OOCCH_3)_2]$ (**1b**)/Si(111) showed the evenly distributed complex on the silicon surface. The copper content was the biggest (1.44%) when spin rate was set at 1100 rpm. Additionally, some crystallites were observed. The layers of (**1b**)/Si obtained at the other spin speeds (900, 1000 and 2000 rpm) exhibited lowest copper content (about 0.5%). Moreover, in these cases, the discontinuity of the materials (1000 and 2000 rpm) was noted.

For the $[Cu(en(pyca)_2)(OOCCH_3)_2]$ (**1b**)/Si and $[Cu(en(pyca)_2)Cl_2]$ (**1a**)/Si layers, the surface roughness (R_q - the root mean square roughness) was the highest when the speed was set at 900 rpm (39.3 nm) for (**1a**)/Si or 1100 rpm (12 nm) for (**1b**)/Si. Increasing the spin speed to 2000 rpm resulted in a lowering of the surface roughness, giving a relatively smooth material (R_q = 14.7 nm for (**1a**) and 7.26 nm for (**1b**)). Reducing the rotation speed gave a layer of (**1b**)/Si with some structures sticking out of the surface. Additionally, the latter materials were irregularly covered by the compound.

Similar to the (**1b**)/Si and (**1a**)/Si materials, the lowest roughness of $[Cu(en(4Him)_2)Cl_2]$ (**2a**)/Si was observed at the spin speed of 2000 rpm (R_q = 25.8 nm). The complex was evenly spread on the Si(111) substrate. While, in contrast to (**1b**)/Si and (**1a**)/Si, in (**2a**)/Si lowering the spin speed did not cause important changes in the surface roughness. In the case of $[Cu(en(dmbaH)_2)Cl_2]$ (**3a**)/Si, the AFM analysis showed that complex (**3a**) is evenly arranged on Si substrate (figure 4). The compound formed islands of different heights, resulting in a flat surface (R_q = 19.5 nm, 1000 rpm). However, empty spaces in the surface were observed, which indicated layer discontinuity. Other spin speeds led to materials of the lowest roughness and uniform layers.

The above results suggest that the quality of the layer (uniformity, roughness) can be optimized by the variation of spin speed. In conclusion, layers obtained with

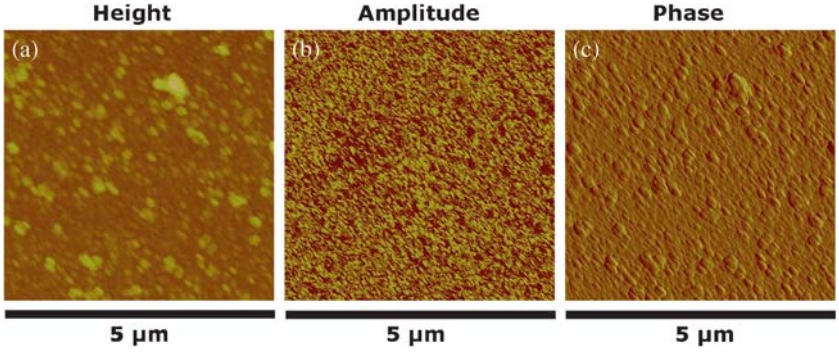

Figure 4. AFM images of $[Cu(en(dmbaH)_2)Cl_2]$ (**3a**)/Si (1000 rpm, time 30 s).

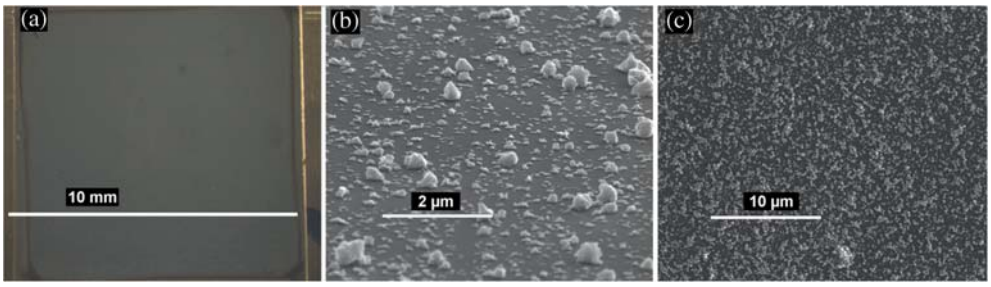

Figure 5. The ZnO layers: (a) optical microscopy and (b: cross-section) SEM images of sample **A4** (3000 rpm, 3 min); (c) SEM image of sample **A6** (5000 rpm, 3 min).

spin coating method are, in general, thin and homogeneous with complexes uniformly spread over the substrate surface.

The best parameters for the spin coating process which provide smooth, thin and homogeneous copper(II) materials with complexes uniformly spread over the substrate surface were: spin speed of 900, 1100 or 2000 rpm for 30 s depending on the precursor used. The layers reveal that the total thickness of film does not exceed 100 nm.

3.5 *[Cu(en(4Him)$_2$)Cl$_2$] (**2a**)/ZnO/Si and [Cu(en(dmbaH)$_2$)Cl$_2$] (**3a**)/ZnO/Si thin films*

The zinc oxide layers were examined by optical microscopy (OM), SEM and AFM. In most cases, we observed uniform coated surfaces (figure 5a,c). It was noticed that the inorganic material was deposited both as separate grains and agglomerates composed of several nanoparticles (figure 5b). The AFM analysis of sample **A4** layers reveals that the total thickness of film does not exceed 500 nm.

In the case of the mixed layers, the copper complex and ZnO form aggregates and grains which pointed to porous nature of the layer (figure 6a,b). The total thickness of the layer does not exceed 700 nm. The mapping analysis indicated uniformly deposited copper complex and ZnO on the silicon surface (figure 6c). Similar situation for layers of complexes was observed.[55] Spin coated thin films of Cu, Co, Ni or Pb complexes with different tetraazaporphyrine derivatives on glass or quartz substrates had also shown porous structures with disordered array of island aggregation and thickness between 40 and 250 nm.[56–58] Those films, because of their porous nature, showed gas sensing behavior. Summarizing, the multistage coating process allows obtaining thin, uniform copper complex-zinc oxide mixed layers.

3.6 *Fluorescence properties of layers*

The fluorescence properties of the prepared layers were studied. [Cu(en(pyca)$_2$)Cl$_2$] (**1a**)/Si, [Cu(en(pyca)$_2$)(OOCCH$_3$)$_2$] (**1b**)/Si and [Cu(en(dmbaH)$_2$)Cl$_2$] (**3a**)/Si materials exhibited the highest fluorescence intensity between 472 and 503 nm from intraligand $\pi \rightarrow \pi^*$ transitions ($\lambda_{ex} = 382$ nm). The highest-intensity of emission band was noted for layers with relatively low roughness (1100 rpm for (**1a**)/Si and 900 rpm for (**1b**)/Si). Similar behavior was registered by us for layers of copper(II) complexes with Schiff bases derived from 2-(2-aminoethyl)pyridine.[23] Materials formed with [Cu(en(4Him)$_2$)Cl$_2$] (**2a**)/Si were excited at 365 nm. In all cases, the emission from intraligand $\pi \rightarrow \pi^*$ transitions at 462 nm was observed. A substantially higher intensity of the fluorescence band for (**2a**) was registered for layer obtained at 1000 rpm. The above results indicate that the copper layers exhibit emission and that uniformly distributed film on substrate increases the emission band intensity.

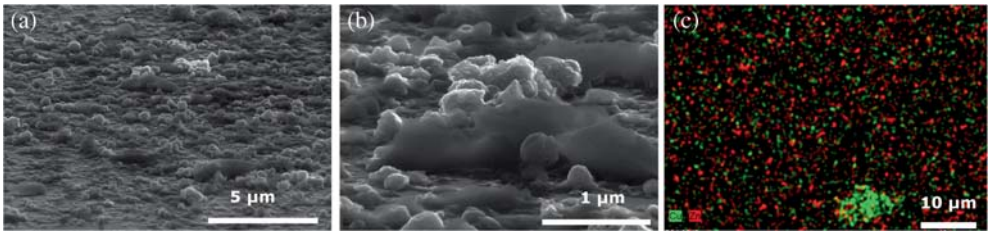

Figure 6. The SEM/EDS analysis of [Cu(II)((en)(4Him)$_2$)Cl$_2$] (**2a**)/ZnO/Si: SEM (a, b; cross-section); EDS mapping (c) (Cu - green and Zn - red areas).

The fluorescence properties of mixed copper complex/ZnO/Si films were studied as well. It is known that ZnO nanoparticles and the Schiff bases exhibit photoluminescence (PL)[32,59] and have varied optical applications.[33] In the PL spectrum of ZnO, typically there are emission bands in the UV and visible regions.[60] The PL spectrum of ZnO nanorods excited at 320 nm showed two UV emission bands at 356 nm and 382 nm. The emission peak at 356 nm may be attributed to the band gap luminescence as it is blue shifted compared to the optical absorption. The near-band edge (NBE) emission peak at 382 nm is assigned to the recombination of free excitons.[61] In addition, a broad shoulder in the range 400–425 nm and very weak defect-related blue emissions at 445, 453 and 470 nm also appeared. Blue emission bands in ZnO nanostructures were also reported[62–65] which are associated with various intrinsic or extrinsic lattice defects. In order to check the influence of the copper complexes on the PL properties of the ZnO layer, the emission spectra of ZnO/Si, $[Cu(en(4Him)_2)Cl_2]$ (**2a**)/ZnO/Si, $[Cu(en(dmbaH)_2)Cl_2]$ (**3a**)/ZnO/Si, $[Cu(en(dmbaH)_2)Cl_2]$ (**3a**)/Si, and $[Cu(en(4Him)_2)Cl_2]$ (**2a**)/Si were recorded. The intensity of the fluorescence band was the lowest for the copper(II) complex/Si layers. On the other hand, the highest intensity of the emission band was exhibited by the ZnO/Si film. For the ZnO nanopowder layers mixed with copper(II) complexes $[Cu(II)(en(4Him)_2)Cl_2]$ (**2a**)/ZnO/Si and $[Cu(en(dmbaH)_2)Cl_2]$ (**3a**)/ZnO/Si, quenching of the PL band of ZnO at 440 nm was observed (λ_{ex} = 330 nm, figure 7). Additionally, because of the low intensity of the fluorescence, a band coming from Rayleigh scattering at 659 nm and 649 nm for $[Cu(II)((en)(4Him)_2)Cl_2]$ (**2a**)/ZnO/Si and $[Cu(en(dmbaH)_2)Cl_2]$ (**3a**)/ZnO/Si, respectively, were registered.[66] The quenching of fluorescence by Cu(II) ion can be explained by process such as magnetic perturbation or redox activity.[67–69]

3.7 *The indentation of the layers*

Preliminary indentations were performed on uncoated silicon substrates (Si(100)), Cu(complex)/Si and Cu(complex)/ZnO (**A4**)/Si wafers (figure 8). The calculated indentation hardness (HIT) and the indentation modulus (EIT) for silicon ranged from 10.754 to 11.561 GPa and from 172.20 to 191.4 GPa, respectively, depending on the maximal load and loading rate values. The obtained values correspond well with comparable literature data.[70,71] In the case of fabricated layers, the elastic modulus was, in general, similar to silicon substrate while hardness values were apparently lower than that for Si(111). Moreover, we observed a significant decrease of both mechanical parameters for samples deposited at lower rotation speed coexisting with longer deposition times (samples **I** and **IV**). The application of such coating parameters resulted in thicker layers, which obviously had serve impact on the mechanical properties of our composites. Additionally, the characteristic for monocrystalline silicon the pop-out phenomenon, which appeared during unloading for most measurements, was observed.[72] It may be related to a substantial effect of the substrate on the overall hardness measure. In general, the hardness response

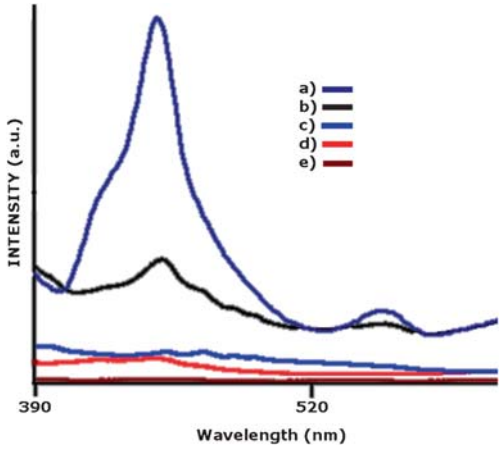

Figure 7. The photoluminescence spectra of (a) ZnO/Si (2000 rpm, 3 min), (b) $[Cu(en(4Him)_2)Cl_2]$ (**2a**)/ZnO/Si (1500 rpm, 1 min/3000 rpm, 3 min), (c) $[Cu(en(dmbaH)_2)Cl_2]$ (**3a**)/ZnO/Si (2000 rpm, 10 min/3000 rpm, 3 min), (d) $[Cu(en(dmbaH)_2)Cl_2]$ (**3a**)/Si (4000 rpm, 10 min), (e) $[Cu(en(4Him)_2)Cl_2]$ (**2a**)/Si (1500 rpm, 5 min).

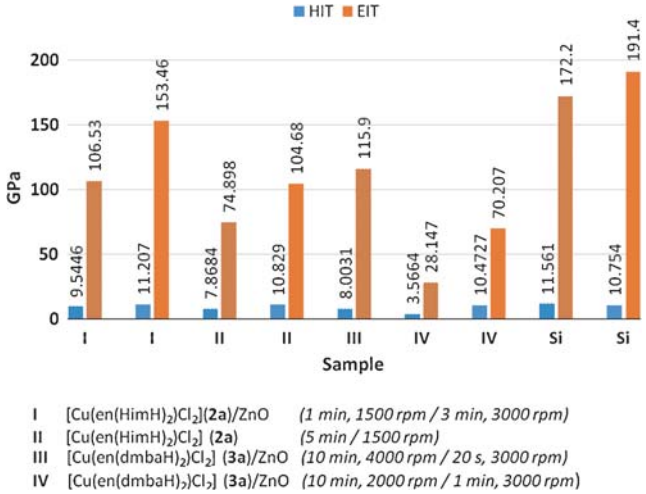

Figure 8. The hardness (HIT) and elastic modulus (EIT) values of fabricated layers registered under the following conditions: loading rate 200 mN/min, max. load 100 mN (dotted bars) and loading rate 40 mN/min, max. load 20 mN (solid bars).

of "soft film on hard substrate type" results from microstructures of layer substrate and physical phenomena, such as the indentation size effect or cracking around the indent.[73,74] The pileup around the indenter can also occur because of relative softness of deposited layer in comparison to the harder silicon wafer. Due to the complexity of the studied materials, it is difficult at this point to clearly interpret the obtained results.

4. Conclusions

A series of Schiff bases and their copper(II) complexes derived from ethylenediamine and three different aldehydes were obtained. In four cases, the copper ion exists in square planar N_4 geometry distorted from planarity due to coordination with chloride or acetate ions. Only in the case of $[Cu(en(dmbaH)_2)Cl_2]$ the four coordinated copper ion was observed. The optimal parameters of spin coating, resulting in thin layers with equally spread Cu(II) complexes on Si were: 900, 1100 or 2000 rpm spin rate for 30 s. All the Cu(II) compounds as thin film layers exhibit luminescence at λ_{ex} between 365 and 382 nm. The emission bands from intraligand $\pi \rightarrow \pi^*$ transitions were observed in the range between 462 and 503 nm. The highest intensity of these bands was noticed for the layers with more uniformly placed compounds. The studies on the material properties and the emission of the layer reveal the fact that the complex can be used as optically active materials.

The use of solution-based copper(II) complex and ZnO precursors provides a facile route to composite organic-inorganic thin layer deposits of well-defined thickness. The structure of these films can be controlled *via* appropriate choice of precursor and processing conditions. In the case of ZnO deposition on silicon substrate, uniform, non-continuous coverage but with the island-like aggregates of particles was observed. The mixed layers of copper complex $[Cu(II)((en)(4Him)_2)Cl_2]$ and ZnO nanoparticles exhibited quenching of the ZnO fluorescence band at $\lambda_{em} =$ 440 nm. The analysis of mechanical properties of layers points to decrease in the HIT and EIT values with increasing time of the deposition.

Supplementary Information (SI)

All additional information pertaining to characterization of the ligands using NMR spectroscopy (figures S1–S7), IR spectra of ligands and complexes (figures S8–S18), electronic data (table S1) are given in the supporting information, available at www.ias.ac.in/chemsci.

Acknowledgement

Authors would like to thank the National Science Centre (NCN), Poland for financial support (grant no. *2013/09/B/ST5/03509*).

References

1. Kramer R 1998 *Angew. Chem. Int. Ed.* **37** 772
2. Gaggelli E, Kozlowski H, Valensin D and Valensin G 2006 *Chem. Rev.* **106** 1995
3. Chetana P R, Srinatha B S, Somashekar M N and Policegoudra R S 2016 *J. Mol. Struct.* **352** 1106
4. Rama I and Selvameena R 2015 *J. Chem. Sci.* **127** 671
5. Naeimi A, Saeednia S, Yoosefian M, Rudbari H A and Nardo V M 2015 *J. Chem. Sci.* **127** 1321
6. Lashanizadegan M and Sarkheil M 2012 *J. Serb. Chem. Soc.* **77** 1589
7. Amendola V, Fabbrizzi L, Gianelli L, Maggi C and Mangano C 2001 *Inorg. Chem.* **40** 3579
8. Chen C H and Shi J 1998 *Coord. Chem. Rev.* **171** 161
9. Sanchez C, Rozes L, Ribot F, Laberty-Robert C, Grosso D, Sassoye C, Boissiere C and Nicole C 2010 *C. R. Chim.* **3** 13
10. Brauer B, Zahn D R T, Ruffer T and Salvan G 2006 *Chem. Phys. Lett.* **432** 226
11. Ruzgar S and Caglar M 2015 *J. Nanoelectr. Optoe.* **10** 717
12. Che C M, Chan S C, Xiang H F, Chan M C W, Liu Y and Wang Y 2004 *Chem. Commun.* 1484
13. Chang K H, Huang C C, Liu Y H, Hu Y H, Chou P T and Lin Y C 2004 *J. Chem. Soc. Dalton Trans.* 1731
14. Ghosh R, Rahaman S H, Lin C N, Lu T H and Ghosh B K 2006 *Polyhedron* **25** 3104
15. Hu Y, Gao X, Di C, Yang X, Zhang F, Liu Y, Li H and Zhu D 2011 *Chem. Mater.* **23** 1204
16. Sorar I, Şener M K, Tepehan F Z, Gül A and Koçak M B 2008 *Thin Solid Films* **516** 2894
17. Ting-Ting W, He Zhi-Qun, Xiao-Pan Z, Yong-Sheng W, Chun-Xiu Z and Wen-Guan Z 2007 *Optoelectron. Lett.* **3** 43
18. Qiu W, Hu W, Liu Y, Zhou S, Yu Xu and Zhou D 2001 *Sens. Actuators, B* **75** 62
19. Sirimanne P M, Rusop M, Shirata T, Soga T and Jimbo T 2003 *Mater. Chem. Phys.* **80** 461
20. Jakob A, Rüffer T, Ecorchard P, Walfort B, Körbitz K, Frühauf S, Schulz S E, Gessner T and Lang H 2010 *Z. Anorg. Allg. Chem.* **636** 1931
21. Barwiolek M, Szlyk E, Lis J and Muziol T 2011 *Dalton Trans.* **40** 11012
22. Barwiolek M, Szlyk E, Surdykowski A and Wojtczak A 2013 *Dalton Trans.* **42** 11476
23. Barwiolek M, Szlyk E, Berg A, Wojtczak A, Muziol T and Jezierska J 2014 *Dalton Trans.* **43** 9924
24. Gupta S K, Joshi A and Kaur M 2010 *J. Chem. Sci.* **122** 57
25. Lin B, Fu Z and Jia Y 2001 *Appl. Phys. Lett.* **79** 943
26. Drmosh Q A, Rao S G, Yamani Z H and Gonda M A 2013 *Appl. Surf. Sci.* **270** 104
27. Khanlary M R, Hajinorozi A and Baghshahi S 2015 *J. Inorg. Organomet. Polym.* **25** 1521

28. Heredia E, Bojorge C, Casanova J, Cánepa H, Craievich A and Kellermann G 2014 *Appl. Surf. Sci.* **317** 19
29. Reddy A J, Kokila M K, Nagabhushana H, Rao J L, Shivakumara C, Nagabhushana B M and Chakradhar R P S 2011 *Spectrochim. Acta Part A* **81** 59
30. Singh A K, Viswanath V and Janu V C 2009 *J. Lumin.* **129** 874
31. Xin M, Hu L Z, Liu D-P and Yu N-S 2014 *Superlatt. Microstr.* **74** 234
32. Sharma K P, Kumar M and Pandey A C 2011 *J. Nanopart Res.* **13** 1629
33. Chow L, Lupan O, Chai G, Khallaf H, Ono L K, Cuenya B R, Tiginyanu I M, Ursaki V V, Sontea V and Schulte A 2013 *Sens. Actuators, A* **189** 399
34. Oliver W C and Pharr G M 1992 *J. Mater. Res.* **7** 1564
35. Gullotti M, Pasini A, Fantucci P, Ugo R and Gillard D 1972 *Gazz. Chim. Ital.* **102** 855
36. Smith H E, Neergaard J R, Burrows E P and Chen F M 1974 *J. Am. Chem. Soc.* **96** 2908
37. Lever A B P 2006 In *Inorganic Electronic Spectroscopy* (Hoboken: Wiley-Interscience)
38. Roy S, Choubey S, Bhar K, Khan S, Mitra P and Ghosh B K 2013 *J. Mol. Struct.* **1051** 328
39. Rogness D C, Markina N A, Waldo J P and Larock R C 2012 *J. Org. Chem.* **77** 2743
40. Ogden M D, Meier G P and Nash K L 2012 *J. Solution Chem.* **41** 1
41. Abherve A, Clemente-Juan J M, Coronado M, Boonmak E J and Youngme S 2014 *New J. Chem.* **38(5)** 2105
42. Khalaji A D, Mighani H, Gholinejad M, Grivani G, Akerdi S, Fejfarova J K and Dusek M 2013 *J. Struct. Chem.* **54** 774
43. Günther H 2013 In *NMR Spectroscopy Basic Principles, Concepts, and Applications in Chemistry* (New York: John Wiley)
44. Baillie M J, Brown D H, Moss K C and Sharp D W 1968 *J. Chem. Soc. A* **12** 3110
45. Nakamoto K 2009 In *Infrared and Raman Spectra of Inorganic and Coordination Compounds* 6th ed. (New York: John Wiley)
46. Deacon G B and Phillips R J 1980 *Coord. Chem. Rev.* **33** 227
47. Morzyk-Ociepa B and Michalska D 2003 *Spectrochim. Acta Part A* **59** 1247
48. Cotton F A and Wilkinson G 1988 In *Advanced Inorganic Chemistry* 5th ed (New York: John Wiley)
49. R D Gillard and J A Mc Cleverty (Eds.) 1987 *Comprehensive Coordination Chemistry* (Oxford: Pergamon) Vol. 2 p.716
50. Bitenc M, Marinšek M and Orel Z C 2008 *J. Eur. Ceram. Soc.* **28** 2915
51. Hsieh Ch-H 2007 *J. Chin. Chem. Soc.* **54** 31
52. Singh S, Barick K C and Bahadur D 2013 *J. Mater. Chem. A* **1** 3325
53. Anžlovar A, Kogej K, Orel C Z and Žigon M 2014 *Cryst. Growth Des.* **14** 4262
54. Jakob A, Rüffer T, Schmidt H, Djiele P, Körbitz K, Ecorchard P, Haase T, Köhse-Hoinghaus K, Frühauf S, Wächtler T, Schulz S, Gessner T and Lang H 2010 *Eur. J. Inorg. Chem.* 2975
55. Komino T, Matsuda M and Tajima H 2009 *Thin Solid Films* **518** 688
56. Bin W, Li Z, Zuo X, Wu Y, Wang X, Chen Z, He Ch, Duan W and Gao J 2010 *Sens. Actuators, B* **149** 362
57. Wang B, Chen Z, Zuo X, Wu Y, He Ch, Wang X and Li Z 2011 *Sens. Actuators, B* **160** 1
58. Wang B, Zhou X, Wu Ch, He Ch and Zuo X 2012 *Sens. Actuators, B* **161** 498
59. Babikier M, Wang D, Wang J, Li Q, Sun J, Yan Y, Yu Q and Jiao S 2014 *Nanoscale Res. Lett.* **9** 199
60. Kundu T K, Karak N, Barik P and Saha S 2011 *Int. J. Soft Comput. Eng. (IJSCE)* **1** 19
61. Chen S J, Liu Y C, Shao C L, Mu R, Lu Y M, Zhang J Y, Shen D Z and Fan X W 2005 *Adv. Mater.* **17** 586
62. Zhang D H, Wang Q P and Xue Z Y 2003 *Appl. Surf. Sci.* **207** 20
63. Du G H, Xu F, Yuan Z Y and Tendeloo G V 2006 *Appl. Phys. Lett.* **88** 243101
64. Park J H, Muralidharan P and Kim D K 2009 *Mater. Lett.* **63** 1019
65. Li Y, Xu L, Li X, Shen X and Wang A 2010 *Appl. Surf. Sci.* **256** 4543
66. Lakowicz J R 2006 In *Principles of Fluorescence Spectroscopy* 3th ed. (New York: Springer)
67. Chen X-M and Liu G-F 2002 *Chem. Eur. J.* **8** 4811
68. Varnes A W, Dadson R B and Wehry E L 1972 *J. Am. Chem. Soc.* **94** 946
69. Kemlo J A and Sheperd T M 1977 *Chem. Phys. Lett.* **47** 158
70. Hess P 1996 *Appl. Surf. Sci.* **106** 429
71. Kim M T 1996 *Thin Solid Films* **283** 13
72. Chang L and Zhang L C 2009 *Acta Mater.* **57** 2148
73. Yoon H-K and Yu Y-S 2005 *Int. Symp. on Electronics Materials and Packaging EMAP* 11–14.12.2005, **2005** 169
74. Korsunsky A M, McGurk M R, Bull S J and Page T F 1998 *Surf. Coat. Technol.* **99** 171